Phonon echoes in a glass at low temperatures

John E. Graebner and Brage Golding
Bell Laboratories, Murray Hill, New Jersey 07974
(Received 22 August 1978)

Coherent acoustic echoes are generated in fused silica glass at very low temperatures by a sequence of short acoustic pulses that interact with the intrinsic two-level configurational systems of the glass. Coherent effects are observable below $T \approx 100$ mK, where the two-level-system phase memory time T'_2 is long compared to the acoustic pulse length, typically 100 nsec. The dependence of spontaneous (two-pulse) and stimulated (three-pulse) echo amplitude on the amplitude, width, frequency, and separation time of the generating pulses has been studied in the frequency range 0.7–1.5 GHz and at temperatures of 18–80 mK. The area of the generating pulses is shown to be the relevant descriptive parameter. The value of the area that produces maximum echo amplitude is used to deduce the average value of the deformation potential γ_L which couples a two-level system and a longitudinal acoustic wave, with the result $\gamma_L = 1.5 \pm 0.4$ eV. The two-pulse echo decay time is 16 μsec at 18 mK and varies as T^{-2}. This behavior may be understood in terms of spectral diffusion arising from elastic dipolar interactions between resonant and nonresonant two-level systems. The three-pulse echo decay is not exponential, but may be characterized by an initial decay time of 100 μsec at 0.7 GHz and 18 mK. This is in reasonable agreement with a direct-process thermal equilibration time T_1 calculated from the present value of γ_L. At higher temperatures, the decay rate is faster than indicated by the direct process, and may be understood semiquantitatively in terms of spectral diffusion.

PACS numbers: 62.80. + f, 43.35. + d, 61.40.Df

I. INTRODUCTION

The large heat capacity and low thermal conductivity of glasses below 1 K (Refs. 1–3) can be understood in terms of a broad distribution of two-level configurational systems which are intrinsic to the glassy state.[4-6] The microscopic nature of a two-level system is not well understood but it is assumed to be an atom or a group of atoms which resides in a double-well potential with energy splitting E between the two lowest energy levels. A roughly constant density of states for $0.02 \leq E/k_B \leq 1$ K due to the random environment of the two-level systems accounts for the approximately linear specific heat. The thermal-phonon mean free path is limited by resonant absorption by these two-level systems, yielding the low thermal conductivity. The observed attenuation of high-frequency acoustic pulses is intensity dependent, exhibiting saturation[7,8] at high acoustic inputs which is consistent with the two-level model. The predictions of the model for the temperature and frequency dependence of the unsaturated absorption have been verified experimentally.[9,10] Several reviews of phonon propagation in glasses at low temperature have appeared recently.[11,12]

At low enough temperatures the phase memory time of these two-level systems becomes equal to or greater than the pulse length and coherent effects become observable. Phonon echoes, the acoustic analog of spin echoes[13] or photon echoes,[14] have been observed[15] and the present report provides a more complete description of that work. We begin with a brief account of the two-level model of a glass and the conditions under which one might expect to observe phonon echoes.[16] The application of this technique to the measurement of deformation potentials and relaxation times is described, followed by a discussion of the results and how they relate to previous measurements.

In the two-level tunneling model,[4-6] a two-level system of mass m is represented by a double-well potential with energy asymmetry Δ, barrier height V, and generalized-coordinate separation distance d. A random distribution of these parameters results in some two-level systems with sufficient wave-function overlap between the two wells to allow tunneling to occur, i.e., with tunneling energy $E = (\Delta^2 + \Delta_0^2)^{1/2}$, where $\Delta_0 = \hbar\omega_0 e^{-\lambda}$ and $\lambda = \hbar^{-1} d(2mV)^{1/2}$. $\hbar\omega_0$ is on the order of 10 meV, and the model restricts the wave-function overlap parameter λ to $\lambda_{\min} < \lambda < \lambda_{\max}$, where $\lambda_{\min} = \ln(\hbar\omega_0/E)$ and $\lambda_{\max}$ is some cutoff value. The thermal relaxation rate of two-level systems with tunneling energy E, assuming a one-phonon process, is[4,6]

$$T_1^{-1}(E,\lambda) = \left(\frac{\gamma_L^2}{v_L^5} + \frac{2\gamma_T^2}{v_T^5}\right) \frac{E^3 e^{-2(\lambda-\lambda_{\min})}}{2\pi\hbar^4\rho} \coth\left(\frac{E}{2k_BT}\right), \tag{1}$$

where the subscripts refer to longitudinal- and transverse acoustic polarizations, v is the acoustic velocity, and ρ is the mass density. γ_i is the deformation potential coupling a two-level system with strain e_i. The fastest relaxation occurs

for $\lambda = \lambda_{min}$ which corresponds to $\Delta = 0$, i.e., the symmetric double-well potentials. The specific heat is influenced by all the two-level systems having relaxation times shorter than the duration of the measurement. The acoustic density of states $\tilde{n}$ appears experimentally[7,9,11] to be lower than the specific heat density of states n_0 and can be explained to a first approximation by assuming that only the approximately symmetric two-level systems are effective in the acoustic experiments.[11,17] The deformation potential is actually a tensor quantity, and the scalar γ represents a suitable average of the various components.[17,18] Furthermore, γ is assumed for simplicity to be the same for all two-level systems.

Because of the formal equivalence among quantum mechanical systems with two levels,[19] it is useful to write the Hamiltonian in the familar form for a spin-$\frac{1}{2}$ particle and make use of the extensive literature on resonance physics. One can write[11,20]

$$H = H_0 + H_1 = \tfrac{1}{2}E\sigma_z - (M\sigma_x + \tfrac{1}{2}D\sigma_z)e \qquad (2)$$

with

$$\sigma_x = \begin{pmatrix} 0 & 1 \\ 1 & 0 \end{pmatrix} \text{ and } \sigma_z = \begin{pmatrix} 1 & 0 \\ 0 & -1 \end{pmatrix}.$$

H_0 gives the static splitting and H_1 describes the interaction with a strain e. Within the tunneling model, the coupling parameters M and D are given by $\gamma\Delta_0/E$ and $2\gamma\Delta/E$, respectively. One can define a pseudopolarization vector $\vec{P}_i$ analogous to the magnetization vector of a system of spins. The expectation values of P_x and P_y are now related not to the transverse components of spin, but to the components of stress which are in phase and out of phase with the applied strain. Since in our case the wavelength is much smaller than the sample dimension, $\langle P_i \rangle$ must satisfy the coupled Bloch and wave equations. In this sense the present experiment is more analogous to light traveling through a resonantly absorbing medium[21] than to magnetic spin resonance. As in either case, however, the Bloch equation can be written with a thermal equilibration time T_1, as well as a homogeneous transverse relaxation time T_2, where

$$(T_2')^{-1} = (2T_1)^{-1} + (T_\phi)^{-1}$$

and T_ϕ is the phase memory time due to all processes which do not cause transitions between the two levels. T_ϕ may be determined, for example, by interactions among the two-level systems. The total linewidth

$$(T_2)^{-1} = (T_2')^{-1} + (T_2^*)^{-1}$$

due to both homogeneous and inhomogeneous contributions is very large ($T_2^* \approx 0$) because of the broad range of energy splittings. The two-level systems which are active in the present experiments are only those lying within the spectrum of the acoustic pulse. In the incoherent regime (pulse length $\tau \gg T_2'$), the effect of the pulse interacting with the medium can be described by the *populations* of the upper and lower levels. As τ is decreased or T_2' increased, a smooth transition is made from the incoherent to the coherent regime ($\tau \ll T_2'$) where the phase as well as occupation number is important. The response of the medium is extremely nonlinear and one expects coherent effects such as echoes[14] and self-induced transparency[22,23] which are completely analogous to the optical case. Evidence for self-induced transparency[24,25] will be the subject of a later publication. A significant difference between the present acoustic experiment and a resonant optical experiment is that the acoustic pulse undergoes total reflection at the surface of the sample. As will be seen, the ensuing multiple exposure of the two-level systems to the reflected pulses complicates the interpretation of the data.

All data presented here are obtained with a single piezoelectric transducer generating either the two-pulse or the three-pulse sequence shown in Fig. 1. The first two pulses R_{10} and R_{20} with separation time τ_{12} propagate down and back along the same physical path in the sample. R_{ij} refers to the jth reflection of the ith input pulse, while τ_{kl} refers to the time interval between the kth and lth input pulses. After one round trip (2.2 μ sec) the reflected pulses R_{11} and R_{21} are detected at the transducer. These signals we call *reflections*

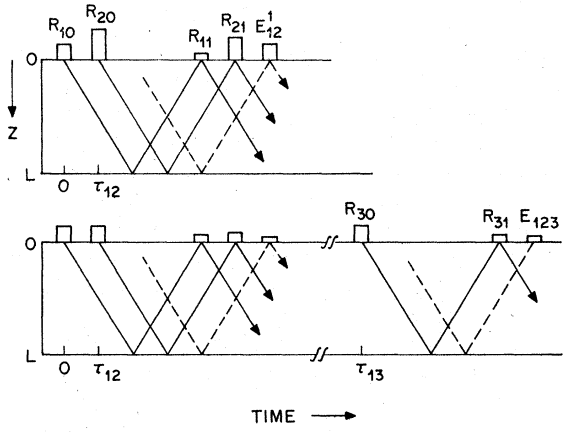

FIG. 1. Schematic diagram of the acoustic pulse sequences for generation of the spontaneous echo E_{12}^1 (top) and stimulated echo E_{123} (bottom). Only the envelopes of the rf pulses are shown. $L = 0.64$ cm, so that the round trip time for longitudinal acoustic pulses in fused silica is 2.2 μsec.

reserving the term *echo* for the pulse E_{12}^1, detected a time τ_{12} after the second reflected pulse. The echo does not correspond directly to any pulse injected at the transducer but is an acoustic pulse which occurs at a spacing τ_{12} after R_{21}. E_{12}^1 is referred to as the two-pulse, or spontaneous, phonon echo.[15] The three-pulse sequence begins in a similar way, but at a later time τ_{13} (5–500 μsec) a third pulse R_{30} is injected, and an echo E_{123} appears at a time after its reflection R_{31}, which is again just τ_{12}, the separation of the *first* two pulses. E_{123} is referred to as the three-pulse, or stimulated, phonon echo. The mechanism of echo formation is formally identical to that which produces photon echoes.[14,26] As with all coherent echo phenomena, the most useful description of a pulse is in terms of its area θ. The acoustic pulse can be described by a traveling strain wave $e = e_0 \cos(\omega t - kz)$. By comparison of Eq. (2) with the usual rotating coordinate treatment of the Bloch equations, we find that the nutation frequency $\omega_1 = Me_0/\hbar$, which is equal to $\gamma e_0/\hbar$ for symmetric two-level systems ($E = \Delta_0$). The pulse area is therefore defined as

$$\theta \equiv \frac{\gamma}{\hbar}\int_{-\infty}^{\infty} e_0\, dt = \frac{\gamma e_0 \tau}{\hbar}\,, \tag{3}$$

where the last equality is true for a pulse of rectangular envelope. The two-pulse echo can be produced by input pulses of area θ_{10} and θ_{20} within a certain range of values, but is most easily visualized with $\theta_{10} = \frac{1}{2}\pi$ and $\theta_{20} = \pi$. (The subscripts for θ have the same meaning as for R.) For any particular two-level system along the acoustic path which is in resonance with the pulse, the effect of the first pulse is to rotate $\langle P_z \rangle$ by $\frac{1}{2}\pi$ from its equilibrium position along P_z to the P_x–P_y plane. The spread in frequencies $\Delta\omega$ of the excited states, determined in our case by the pulse spectrum $\sim\tau^{-1}$, results in rapid dephasing in the P_x-P_y plane. The second pulse reverses the process so that at a time $2\tau_{12}$ after the first pulse, all two-level systems which have not lost their phase memory are rephased momentarily to add up coherently into an acoustic signal. If the processes which destroy phase memory occur randomly, one would expect the echo to decay as $\exp(-2\tau_{12}/T_2')$. The loss in amplitude of E_{12}^1 as a function of $2\tau_{12}$ is then a measure of T_2'. The contributions of all volume elements along the acoustic path must be combined with proper attention given to phase. The resulting intensity for $\tau_{12} \to 0$, by analogy with the optical case,[14] is

$$\mathcal{I}_{12}^1(\vec{k}, T) = \mathcal{I}_0(T=0) N^2 \sin^2\theta_{10} \sin^4(\tfrac{1}{2}\theta_{20}) F(\vec{k})\,, \tag{4}$$

where $\mathcal{I}_0$ is the radiation strength of a single two-level system at resonance. N is the effective number of two-level systems per unit volume within the pulse bandwidth, $N \approx \bar{n} h \tau^{-1} \tanh(\hbar\omega/2kT)$. The N^2 rather than N dependence distinguishes the echo formation as a coherent rather than incoherent process. $F(\vec{k})$ is the result of summing the contributions from all two-level systems in the path of the beam and is a function which is strongly peaked in the direction of $\vec{k} = 2\vec{k}_2 - \vec{k}_1$, where $\vec{k}_1$ and $\vec{k}_2$ are the wave vectors of the first and second pulses, respectively. The echo thus propagates in the forward direction since $\vec{k}_1 = \vec{k}_2$, and maximum echo intensity occurs for a $\frac{1}{2}\pi$, π sequence.

The three-pulse echo formation may be viewed as a storing of information in the population spectrum of the two-level systems by the first two pulses which is then read out by the third pulse. The first two pulses result in a population spectrum which is the Fourier transform of the first *two* pulses, i.e., the Fourier transform of one pulse deeply modulated[27] at a frequency spacing $\Delta\omega = 2\pi\tau_{12}^{-1}$. This modulation is present as long as spin-lattice relaxation, for example, does not relax the entire spectrum back to thermal equilibrium. The third pulse acts on this complicated population spectrum in such a way as to give rise to echo E_{123} after an interval τ_{12} and maximum echo amplitude occurs for a sequence of three $\frac{1}{2}\pi$ pulses. The loss in intensity of echo E_{123} as a function of τ_{13} is then a measure of the effective T_1.

In terms of the measured energy per cm^2 in each pulse, $\mathcal{E}$, the area θ for rectangular pulses may be written

$$\theta = \gamma\hbar^{-1} e_0 \tau = 2\gamma\hbar^{-1}(\mathcal{E}\tau/\rho v^3)^{1/2}\,. \tag{5}$$

$\mathcal{E}$ is related to the acoustic intensity $\mathcal{I}$ by $\mathcal{E} = \mathcal{I}\tau$, and $\mathcal{I}$ ($=\mathcal{I}_{ij}$) is a generic label for the measured intensities of pulses R_{10}, R_{21}, E_{12}^1, etc.

II. EXPERIMENTAL TECHNIQUE

Details of the apparatus have been described previously.[9,12] Briefly, all measurements reported here were obtained with a 0.635-mm cube of Suprasil W(~1.5-ppm OH^-) having a thin-film ZnO transducer (0.8-mm diam) on one of two optically flat and parallel opposite faces. A miniature stub stretcher mounted close to the sample made it possible to tune the non-50-ohm transducer load to the coaxial line, while at the same time providing a metallic thermal ground for the center conductor of the cable. The sample was greased against a Cu block in good thermal contact with the mixing chamber of a ^{3}He–^{4}He dilution refrigerator. Temperature was measured by a Ge resistor on the sample calibrated against a SQUID–CMN (superconducting quantum-interference device–cerium magnesium nitrate) thermometer.[28]

The electrical pulses were obtained by gating an oscillator with diode switches capable of 20-nsec switching times. The pulse was split into two channels, one including the sample and the other a variable attenuator at room temperature. By equalizing the signals from the two channels, the nonlinear response of the glass sample could be measured by comparison with linear elements at room temperature, avoiding problems from nonlinearities in the detection electronics. Distortions of the trailing edge of a pulse due to the video output stage of the 70-MHz i.f. amplifier made the pulse shape an unreliable measure of pulse width. Several other measurements were used to estimate the actual width. The gating pulse applied to the switch was measured directly on an oscilloscope and the average power in the generated pulses was measured as a function of gating pulse width. Additional broadening of the shortest pulses by the tuned stub stretcher was observed by measuring the width of the detected pulse, both on and off the frequency to which the stub stretcher had been tuned. The full widths at half intensity of the acoustic pulses used in the present measurements were estimated to be 65, 115, and 280 nsec, each with an uncertainty of ±10 nsec. The rise and fall times of the pulses were approximately 30 nsec, independent of the pulse width, so that the shortest pulses were roughly Gaussian whereas the longer pulses were more rectangular.

The output of the i.f. amplifier was signal-averaged with a boxcar integrator. The repetition frequency was varied in the range 1–1000 Hz in such a way as to keep the average acoustic power roughly constant as the pulse length or intensity was changed. Even at the lowest temperatures, no bulk heating was registered by the Ge thermometer mounted on the sample.

III. ECHO PRODUCTION

In this section we discuss the dependence of the echo intensity on the intensity and width of the generating pulses. The data enable us to test the relevance of Eq. (4) for the present acoustic echo, as well as to calculate directly the coupling constant.

An x-y recorder trace of the boxcar output (Fig. 2) with two equal input pulses R_{10} and R_{20}, demonstrates the lower attenuation experienced by the second pulse due to the excitation produced by the first. Part of the energy stored in the system from the two generating pulses is returned coherently in the form of an echo E_{12}^1 which in the present example is stronger than R_{11}. Another echo E_{12}^2 is observed after an equal time interval, and we associate this with R_{21} and E_{12}^1 acting as the generating pulses. It is usually weak and we disregard it in the present discussion. The equality of the peak-to-peak separation time of all the pulses in Fig. 2 is characteristic of inhomogeneously broadened systems.[29]

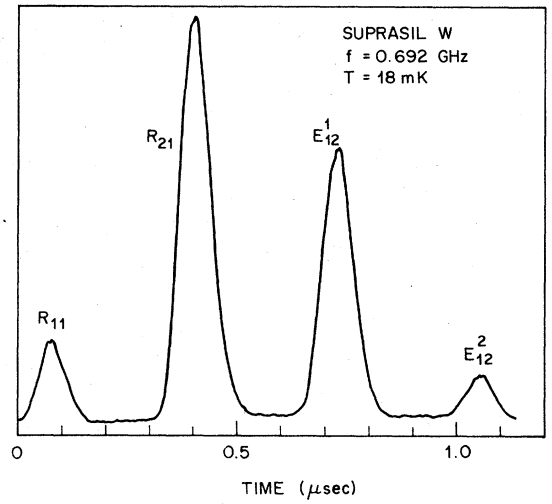

FIG. 2. Boxcar output showing acoustic pulses after one round trip. R_{11} and R_{21} are reflections of the two input pulses while E_{12}^1 and E_{12}^2 are phonon echoes. The equal input pulses have energy density per pulse $\mathcal{E}_{10} = \mathcal{E}_{20} = 4.4 \times 10^{-7}$ erg cm^{-2} and separation time $\tau_{12} = 0.33$ μsec. Pulse width $\tau = 65$ nsec.

The relevance of pulse area as expressed in Eq. (4) can be demonstrated by studying the echo intensity $\mathcal{I}_{12}^1$ as a function of τ, and also of $\mathcal{I}_{10}$ and $\mathcal{I}_{20}$ varied independently. For small and equal input pulses, the echo area $\theta_e \propto \theta_{\text{in}}^3$, according to Eq. (4), so that we have

$$\mathcal{I}_{12}^1 \propto (\theta_{\text{in}}^3)^2/\tau^2 \propto (\mathcal{I}_{10})^3 \tau^4 .$$

$\mathcal{I}_{12}^1$ is plotted in Fig. 3 as a function of $\mathcal{I}_{10}$ for three different values of τ. The lines of slope three are seen to be reasonable representations of the low-power data for all three pulse widths. Furthermore, the vertical spacing of these three lines is such that $\mathcal{I}_{12}^1(\text{const}\mathcal{I}_{10}) \propto \tau^4$. If the maximum echo amplitude occurs at a fixed value of input area, $\theta_{\text{in}}^{\max}$, then since $\mathcal{I}_{10}\tau^2 \propto \theta_{\text{in}}^2$ we expect $\mathcal{I}_{10}(\max\theta_e) \propto \tau^{-2}$. Indeed, the position of maximum echo intensity moves down in $\mathcal{I}_{10}$ as τ^{-2}. Finally, we note that the maximum echo intensity $\mathcal{I}_{12}^1(\max)$ also varies as τ^{-2}, or the square of the bandwidth of the pulse. This is an important result because it demonstrates that the echo intensity varies as the *square* of the number of two-level systems excited by the pulse, as is expected for a coherent mechanism of echo formation.[30]

The results of varying the individual intensities of the generating pulses while keeping the pulse

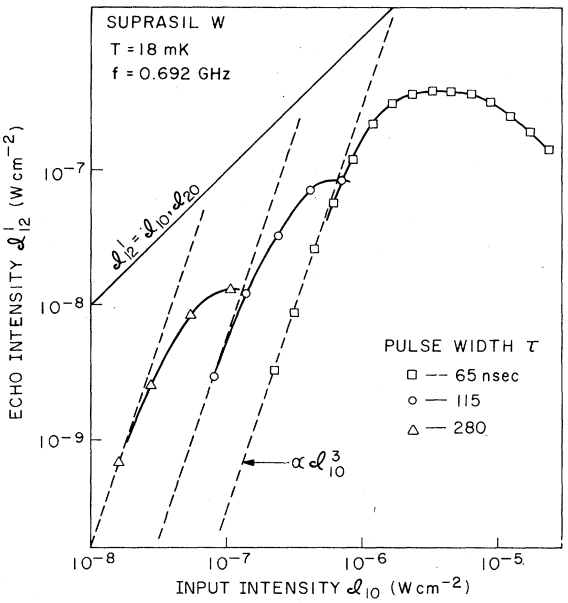

FIG. 3. Spontaneous echo production curves for identical generating pulses at three different widths τ. The solid curves serve only to connect data points. The dashed lines indicate a cubic dependence on input intensity, and the solid line is a reference line along which the echo intensity would be as large as either input pulse.

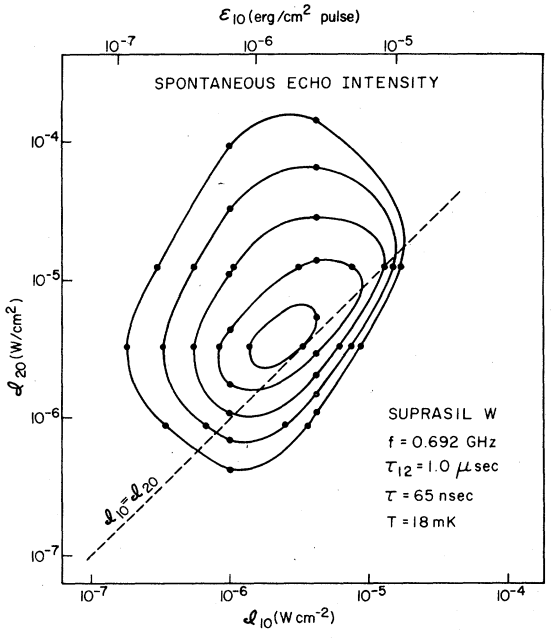

FIG. 4. Contours of equal echo intensity g_{12}^1 for independently varied input intensities g_{10} and g_{20}. The contours are drawn to connect the data points (dots) and occur at 2-dB increments of echo intensity, with the strongest echo occurring at the center of the pattern. Equal input intensities occur along the dashed line and correspond to the data of Fig. 3 for $\tau = 65$ nsec.

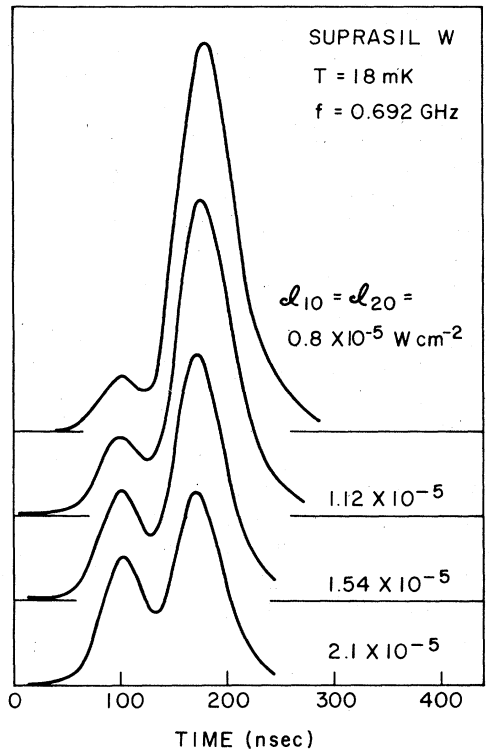

FIG. 5. Echo pulse shapes for large input intensities. Input pulse width $\tau = 65$ nsec.

lengths equal and fixed can be seen in Fig. 4. The contours occur at increments of 2 dB in g_{12}^1, and the position of maximum g_{12}^1 is easily located. The maximum echo *area* θ_e would occur at 2-3 dB lower values of g_{10} and g_{20} because of pulse broadening in this vicinity (see below). The existence of a peak as a function of either g_{10} or g_{20} is clear, and a $\sin^2\theta_{10} \sin^4 \frac{1}{2}\theta_{20}$ behavior is followed quite well up to the peak. For example, along a line of constant g_{10}, g_{12}^1 varies initially as $(g_{20})^2$ at small g_{20} while for constant g_{20}, g_{12}^1 varies initially as g_{10}. Past the peak, however, g_{12}^1 remains considerably higher than suggested by Eq. (4).

At large values of g_{10} and/or g_{20}, the echo splits as shown in Fig. 5. The main echo peak decreases as the input pulse amplitudes are increased, while a precursor appears and grows. If the pulse lengths are not equal to within a few percent, the echo splits into three or more parts. These phenomena have been observed in spin-echo experiments and are due to the different parts of the inhomogeneously broadened resonance line being rotated through different angles. The pulse shapes in Fig. 5 bear a strong resemblance to the calculations and observations in epr echo experiments.[31]

Careful examination of the apparent pulse width

of all the pulses in Fig. 2 shows them to be slightly broader than at higher input intensities. This broadening is greatest (~50%) in the vicinity of maximum echo. The broadening is related to that observed in self-induced transparency[22,25,32] and will be discussed in a later publication.[26] Because of pulse broadening, the maximum intensity is not a good measure of pulse area. In Fig. 6, the pulse area, with broadening taken into account, is shown for the generating pulses and the first echo. At high input levels, the system is linear with a low absorption and very small echo. As the input intensity, or area, is lowered, the echo area goes thru a maximum as the generating pulses are more highly absorbed. At our lowest measurable intensities, $\theta_e \propto \theta_{in}^3$ and the input pulses both experience the same high attenuation, characteristic of a medium which is relatively unaffected by the (weak) pulses traveling through it. The greatest pulse broadening for all three pulses occurs where θ_{11} and θ_{21} are changing most rapidly, and the effect on θ_e is to move the location of the peak to lower input area, θ_{in}, by approximately a factor of 2. Maximum θ_e occurs in Fig. 6 at $\theta_{in}^{max}/\gamma(\text{eV}) = 1.4$. According to Eq. (4), the maximum echo for equal input pulses occurs at $\theta_{in} = \frac{2}{3}\pi$. If the value of θ_{in}^{max} is identified with $\frac{2}{3}\pi$, we obtain $\gamma_L = 1.5 \pm 0.4$ eV, where the uncertainty arises from possible errors in pulse width. Equation (4) does not take into account, however, the dependence of the intensities of the pulses on distance; i.e., the acoustic pulses are traveling, rather than standing waves. The attenuation of the input pulses as they propagate through the sample makes it difficult to estimate the actual area of the pulses as a function of distance. An independent estimate of the area scale can be obtained by approximately reconstructing the intensity as a function of position from θ_{11} and θ_{21} vs θ_{10}, θ_{20} (Fig. 6). For the input level which yields maximum echo, two extreme cases of echo production can be hypothesized. If the echo is assumed to be produced primarily at the beginning of the acoustic path where the pulses are approximately equal, one would expect the input areas to be $\theta_{10} \approx \theta_{20} \approx \frac{2}{3}\pi$ [As in Eq. (4)], again resulting in $\gamma_L = 1.5$ eV. On the other hand, if the echo is produced primarily near the end of the round-trip path, where the areas turn out to be in the ratio 1:2, one would expect the pulse areas at this point to comprise a $\frac{1}{2}\pi$, π sequence, resulting in $\gamma_L = 2.6$ eV. This approximate analysis therefore yields a value for γ_L which is consistent with or somewhat higher than that obtained using Eq. (4).

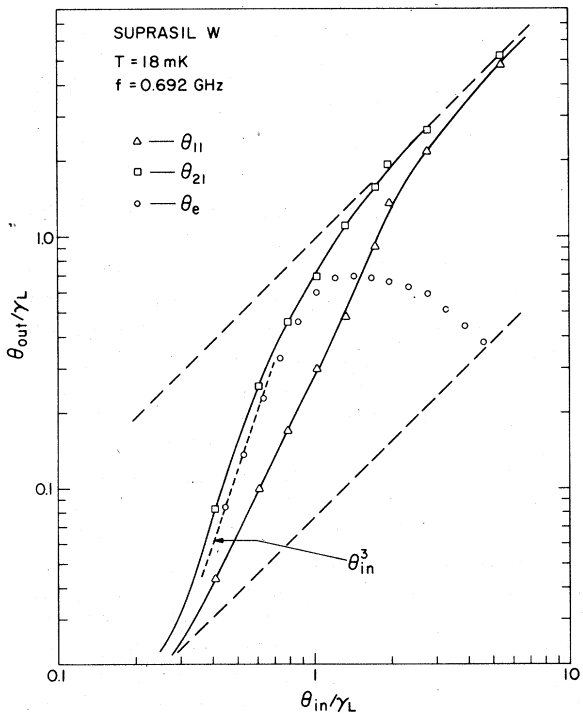

FIG. 6. Area of pulses R_{11}, R_{12}, and E_{12}^1 after one round trip vs area of equal input pulses R_{10} or R_{20}. All areas are plotted as θ/γ_L, a ratio defined in terms of measured quantities in Eq. (5). θ/γ_L is expressed in units of (rad eV^{-1}). Maximum echo production occurs in this transition region between the highly absorbing unsaturated (lower dashed line) and low-absorbing saturated (upper dashed line) conditions. Input pulse widths are both $\tau = 65$ nsec.

Hahn, Shiren, and McCall[33] have obtained equations for the development of pulse areas by application of the area theorem in a *single* pass attenuator. A numerical integration of those equations indicates that the echo area again depends on the cube of the input area, for equal area input pulses, and also goes through a maximum for $\theta_{in} \approx \frac{2}{3}\pi$, supporting the above value, $\gamma_L = 1.5$ eV. There are, however, several discrepancies between the data in Fig. 6 and the predictions of the integrated area equations.[33] First, the calculated echo exhibits a much sharper maximum followed by a zero at π, another weaker maximum at $\theta_{in} \approx 1.5\pi$, a zero at 2π, etc. The observed maximum is much broader and drops off only slowly at higher input area. Second, the calculated area of the echo at the maximum is, after four decay lengths, 2.2 times the input area of either pulse, whereas the measured echo is only 50% of the input area. Third, the maximum echo is calculated to occur at 0.67π which is nearly the same input area as 0.8π, the calculated[32] midpoint of the single-pulse transmission curve (the point at which the attenuation is one-half of the low-power unsaturated value). The measured echo maximum, on the other hand, oc-

curs at 5 dB (a factor of 1.8 in area) *higher* input than the saturation midpoint. The deformation potential calculated from the saturation midpoint[9] (assuming the area equations to apply) is $\gamma_L = 3.2$ eV, compared with 1.5 eV from the position of maximum echo.

There are several possible reasons for the discrepancies. First, the integrated area equations are strictly valid only for input pulses which have a hyperbolic secant shape of the form[22]

$$e(t) = (\hbar/\gamma\tau)\,\mathrm{sech}[(t - z/v)/\tau]\,.$$

While the present pulse shapes are probably intermediate between a rectangular and a hyperbolic secant pulse, several absorption lengths may be required before the input pulses evolve into the latter shape. Secondly, the area equations do not take into account the fact that the pulses travel twice through the same material before being detected. Thus, on the second pass they encounter a medium which is not in thermal equilibrium. Thirdly, the apparent lack of observed zeros and subsidiary maxima at higher inputs may be partially an artifact of the experimental technique. The echo splitting in Fig. 5 may be accompanied by a 180° phase shift between the peaks, so that for equal-height peaks, the net area would be zero. Since θ_e in Fig. 6 is only the area of the main peak, it is probably an overestimate of the total echo area at large inputs, but without phase sensitive detection we cannot justify subtracting the area of the precursor.

There are thus a number of unresolved questions in the interpretation of the echo production curves, as no existing calculation applies to the present case of echo production in a two-pass attenuator. The closest approximation is a calculation[32] of single pulse propagation using numerical solutions of the coupled Bloch and wave equations in the coherent regime, but with the restriction that T_2' is less than the time between passes so that echo production is suppressed. In the absence of a numerical simulation of the present echo production, we take the straightforward interpretation of maximum echo production at $\frac{2}{3}\pi$ as the measure of pulse area, with the resulting deformation potential $\gamma_L = 1.5$ eV. The above considerations suggest that γ_L may in fact be somewhat larger than 1.5 eV, but probably not smaller.

IV. TWO-PULSE ECHO DECAY

We restrict the discussion now to the case of two equal input pulses with $\tau = 65$ nsec, and investigate the decay of the echo amplitude with increasing pulse separation, τ_{12}. The echo amplitude, proportional to $(\mathcal{G}_{12}^1)^{1/2}$, is plotted versus $2\tau_{12}$ in Fig. 7.

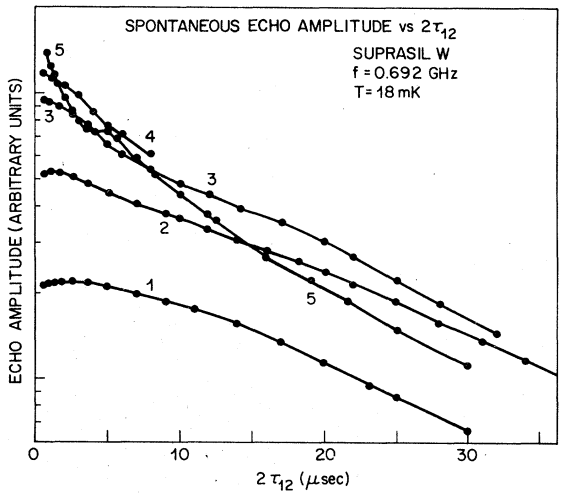

FIG. 7. Decay of spontaneous echo amplitude [proportional to (intensity)$^{1/2}$] as a function of twice the separation time τ_{12}. The input pulses are identical, with pulse length $\tau = 65$ nsec and energy density per pulse $\mathcal{E}_{10} = \mathcal{E}_{20} = 0.22\times10^{-6}$ (1), 0.43×10^{-6} (2), 0.81×10^{-6} (3), 1.05×10^{-6} (4), 2.9×10^{-6} (5) erg cm^{-2}.

The shape of the decay curve depends on the intensity of the input pulses in a complicated way, especially at small $2\tau_{12}$. For input level 1, the echo actually grows initially before decaying, while for input 5 the initial decay is very rapid. The effect is to make the input at which maximum echo occurs somewhat dependent on τ_{12}. At least one feature of decay 5 can be understood due to the first pulse reflecting back and forth several times, repeatedly exciting or de-exciting the same two-level systems. The step beginning at 4.4 μsec occurs as the second pulse changes from traveling just ahead to just behind the first pulse on its second round trip. After this point the direct echo is always coincident with another echo generated by the second pulse, together with the first pulse on its second round trip. The observed echo should therefore be stronger for $\tau_{12} > 2.2$ μsec (one round trip), as observed. Such propagation effects make the initial decay an unreliable measure of the decay rate for a single pass of each pulse. On the other hand, the rates at longer times seem to converge to the same value with a decay time of 16 μsec at 18 mK. Most of the data were taken at an intermediate input level where the long- and short-time decay rates were similar. At higher temperatures the signal was weaker and more difficult to measure but was generally much less intensity dependent than at the lowest temperatures.

The echo decay (see Fig. 8) is roughly exponential at all temperatures measured. The decay time is strongly temperature dependent, varying as T^{-2}

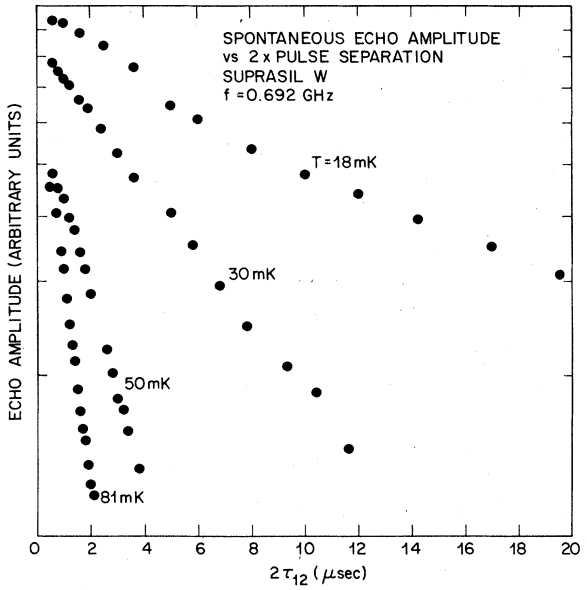

FIG. 8. Decay of spontaneous echo amplitude at four different temperatures. The input pulse intensity is the same as for curve 3 of Fig. 7.

in the range 18–80 mK at 0.692 GHz (see Fig. 9). All of the data discussed up to this point were obtained at 0.692 GHz because of the overall optimum efficiency of the system at this frequency. The system was subsequently retuned at 0.995 and 1.51 GHz with somewhat diminished sensitivity. The results are shown in Fig. 9 with correspondingly larger error bars. For both higher frequencies the decay times agree with the 0.692 GHz data at the higher temperature but remain roughly constant below approximately 40 mK, with the highest frequency data exhibiting the fastest decay rate.

V. THREE-PULSE ECHO

The results reported here for the stimulated echo were obtained with three pulses of identical width and intensity. A detailed study of stimulated echo production, as described above for the spontaneous echo, was not undertaken, but it was noted that maximum echo intensity was obtained with approximately the same input levels, within a factor of 2, as for the spontaneous echo. The strongest echo occurred at $\tau_{13}+\tau_{12}$ but echoes were also noted at $2\tau_{13}-2\tau_{12}$, $2\tau_{13}-\tau_{12}$, and $2\tau_{13}$, in agreement with theory.[13] The echo amplitude at $\tau_{13}+\tau_{12}$ is plotted in Fig. 10 for three different input levels. The general shape of the decay curve does not depend sensitively on the input level, as is the case for the spontaneous echo. The decay is not a simple exponential but begins with a time constant of 100 μsec and gradually changes to a rate half as fast or less. Depending on the range of τ_{13} inspected, one can find a variety of apparent decay times. A dependence on τ_{12} has also been observed in Fig. 11, and is discussed below. The wider sep-

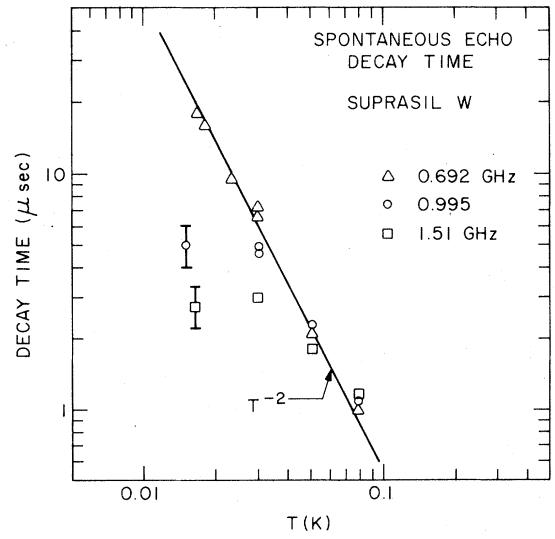

FIG. 9. Spontaneous echo decay time as a function of temperature for three different frequencies. The estimated uncertainty for the 0.692 GHz data is roughly half that shown for the higher-frequency data. The line of slope -2 is drawn to illustrate the T^{-2} dependence of the data at 0.692 GHz.

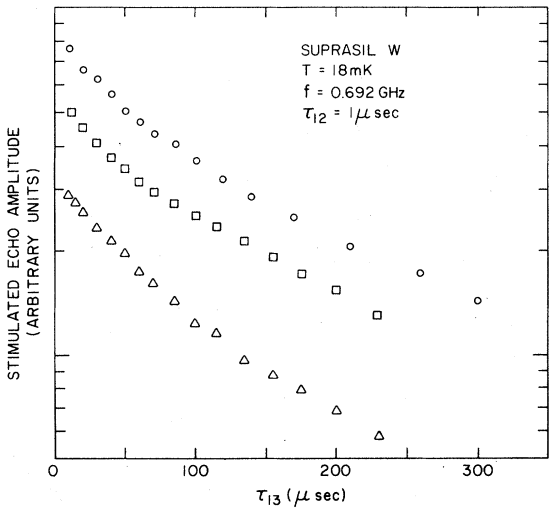

FIG. 10. Stimulated echo decay as a function of separation time between first and third input pulses for three different pulse energy densities: triangles—0.25×10^{-6}, circles—0.95×10^{-6}, and squares—3.7×10^{-6} erg cm^{-2}.

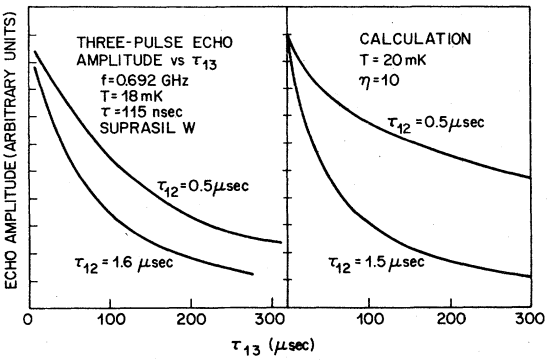

FIG. 11. Stimulated echo decay for two different separation times τ_{12} between the first two input pulses. Results on the left are experimental and on the right are from a calculation by Black and Halperin, Ref. 17, on the basis of spectral diffusion.

aration τ_{12} always yields a faster initial decay of the stimulated echo.

The overall decay rate is very temperature dependent (see Fig. 12) and the amplitude rapidly becomes unmeasurably small above 80 mK. The ini-

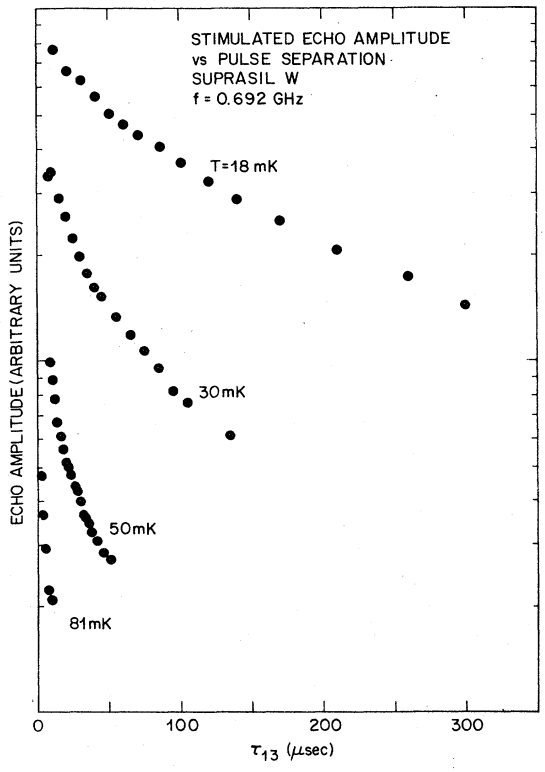

FIG. 12. Stimulated echo decay as a function of pulse separation at four temperatures.

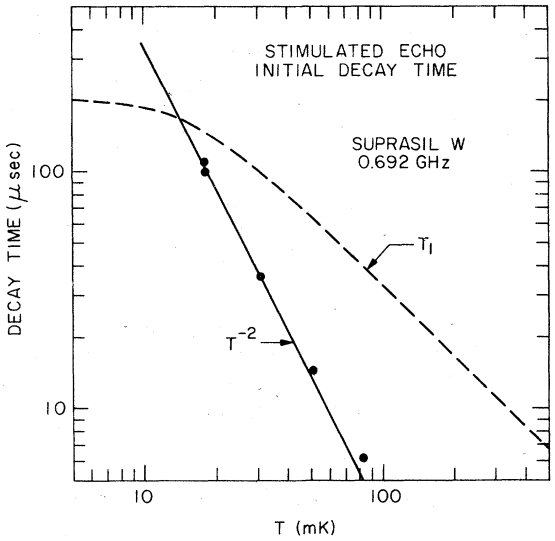

FIG. 13. Decay time of stimulated echo vs temperature from data of Fig. 12. The dashed line is calculated from Eq. (1) with $\gamma_L = 1.5$ eV and $f = 0.692$ GHz.

tial decay times are plotted in Fig. 13, showing a T^{-2} dependence and an initial decay time of 100 μsec at 18 mK. We point out again the possible presence of complicated propagation effects, especially at the higher temperatures where α is small and the generating pulses continue to reflect back and forth across the sample for 10–20 μsec before dying out, and where the measured decay time of the stimulated echo at these temperatures is only ~5 μsec.

VI. DISCUSSION

A. Deformation potential

The value for γ_L determined from maximum echo production, 1.5 eV, falls within a broad range (0.3-5 eV) of previous values, found in fused silica and BK7 borosilicate glass. It is a factor of 2 smaller than an early, rough estimate based on saturation measurements.[7] The 0.3 eV estimate[11] is based on absorption and velocity measurements with the assumption that $\tilde{n} = n_0$. The value of 5 eV is the result of a two-pulse saturation recovery experiment[11] at 0.5 K where, in retrospect, spectral diffusion[17] was probably playing an important but unsuspected role. The present value is only 30% smaller than the value obtained[10] by comparing the saturation curve for single pulse transmission at low temperatures with the curves calculated by Hopf[32] in a two-pass attenuator with $\tau \ll T_2'$.

The product $\tilde{n}\gamma_L^2 = 1.4\times10^8$ erg cm^{-3} from acoustic absorption measurements[9] can be used in

combination with our present independent measurement of γ_L and specific heat results[3] of

$$n_0(E/k_B = 30\ \text{mK}) = 3\times10^{32}\ \text{erg}^{-1}\,\text{cm}^{-3},$$

to obtain $r = \bar{n}/n_0 = 8\%$. That is, only 8% of the two-level systems contributing to the specific heat are well coupled to the acoustic pulses. Using this value of $\bar{n}$, the acoustic energy needed for saturation can be estimated[15] using

$$\mathcal{E}_c = \tfrac{1}{2}\bar{n}\hbar\omega(\hbar\Delta\omega)\tanh(\hbar\omega/2kT)l,$$

where l is the absorption length, with the result $\mathcal{E}_c = 1\times10^{-6}\ \text{erg}\,\text{cm}^{-2}$, in rather good agreement with experiment.[9,11] We conclude, therefore, that this value of γ_L and the resulting value of $\bar{n}$ are consistent with several types of measurements in both the incoherent as well as coherent regimes. Using $\gamma_L = 1.5$ eV and assuming[9] $\gamma_L^2 = 2\gamma_T^2$, Eq. (1) predicts $T_1 = 150$ μsec at $T = 18$ mK and $f = 0.692$ GHz. The temperature dependence of T_1 with these parameters is shown by the dashed line in Fig. 13.

B. Origin of spontaneous echo decay

In view of the large value of T_1 calculated above, the spontaneous echo decay rate at 0.692 GHz is probably dominated by T_ϕ. The most likely source of homogeneous broadening is the interactions between two-level systems. One possible interaction is between two-level systems of the same energy. A two-level system undergoing a change of state can cause a change of state of a nearby two-level system of the same energy through the strain field coupling them. However, the spatial density of those two-level systems within the pulse bandwidth is extremely low ($\sim10^{12}\ \text{cm}^{-3}$), making such interaction unlikely.[11,20] Another possibility which has been explored in some detail is known as the sudden-jump model of spectral diffusion[27,34,35] arising from a $\sigma_z\sigma_z$ coupling between the resonant two-level system and all other two-level systems in the sample, especially those with $E \sim 2k_BT$. The thermal flipping of the latter is coupled elastically to a resonant two-level system and shifts its energy by small random amounts resulting in a kind of spectral diffusion. The effect on the two-pulse echo intensity for a glass has been calculated by Black and Halperin[17] and more recently by Hu and Walker.[36] A nonexponential decay is found which nontheless can be characterized by a time T_ϕ for decay to e^{-1} of the initial amplitude. T_ϕ is calculated[17] to be 14 μsec at 20 mK and varies as T^{-2}, in remarkably good agreement with the present results. The calculation predicts an initial $e^{-a\tau_{12}^2}$ decay, which bears some resemblance to the lowest input power case in Fig. 7. The small input case may, in fact, be the most appropriate decay to compare with a theory which does not take into account propagation effects, since the small input pulses are highly attenuated (Fig. 6) on their first pass, and have negligible amplitude on the return trip. Hu and Walker[36] have suggested that the effect of a reasonably large distribution in λ should be observable as a decay which, at large τ_{12}, is faster than it would be with no distribution in λ. It should be emphasized that this calculation, too, does not take into account the propagation effects inherent in the problem.

The echo decay due to spectral diffusion should be independent of the acoustic frequency.[17] The high-frequency data in Fig. 9 below ~40 mK is therefore puzzling. Qualitatively the data exhibit the behavior expected from a direct-process T_1 relaxation [Eq. (1)] with a nearly temperature-independent ω^{-3} behavior. However, use of the expression $(T_2')^{-1} = (2T_1)^{-1} + (T_\phi)^{-1}$, with T_ϕ taken to be the T^{-2} behavior thought to arise from spectral diffusion, requires the unreasonably high value of $\gamma_L = 5$–6 eV. The peculiar behavior may be connected with some experimental effect due to the higher intrinsic absorption and our reduced sensitivity at the higher frequencies. Measurements over a larger range in frequency and temperature would help to resolve this question.

C. Origin of stimulated echo decay

At the lowest temperature measured, the initial decay time of the stimulated echo, 100 μsec, is remarkably close to the direct-process $T_1 = 150$ μsec based on $\gamma_L = 1.5$ eV. As seen in Fig. 13, however, the agreement rapidly becomes worse at higher temperatures. There are at least three possible reasons for the discrepancy. (a) The effect of spectral diffusion on the three-pulse echo has been calculated[17] and is found to produce a nonexponential decay which qualitatively resembles the data. The initial decay times of the curves in Ref. 17 are difficult to estimate but are within a factor of 2 of the observed values at 18 and 50 mK, exhibiting a somewhat stronger dependence on temperature than T^{-2}. The interpretation in terms of spectral diffusion is given strong support by the dependence of the decay on separation time τ_{12} and the qualitative agreement between theory and experiment seen in Fig. 11. The faster decay for larger τ_{12} can be understood qualitatively as being due to spectral diffusion smearing out the modulated population spectrum more easily for the finer frequency spacing at larger τ_{12}. (b) The long tails of the stimulated echo decay may be evidence for a distribution of relaxation times due to a distribution of tunneling parameters. The symmetric two-level systems may have a distribution of coupling con-

stants, for example, or we may be observing the contributions from more slowly relaxing nonsymmetric two-level systems. (c) The inability of the narrow band of injected phonons to thermalize or escape from the sample rapidly (phonon bottleneck) may give rise to long decay times for the stimulated echo. The problem is complicated by spatial diffusion of the emitted phonons out of the beam volume, which constitutes only 2% of the sample volume. The magnitude and temperature dependence of such a process is difficult to estimate but, as with (b) above, we cannot at this point rule it out as a possible contribution to the stimulated echo decay.

VII. CONCLUSIONS

Our previous observation of phonon echoes in a glass at low temperatures has been extended to include the dependence of echo intensity on the amplitude, width, carrier frequency, and time separation of the generating pulses. The detailed results for the two-pulse echo are in good agreement with the assumption that pulse area is the relevant parameter describing echo formation. The intensity depends on the square of the effective number of radiators, consistent with the assumed coherent aspect of the echo. The spacing of the echo in time is just that expected in the case of inhomogeneous broadening. The location of maximum echo production yields a value for γ_L.

The two-pulse echo decay rate at medium input level is given by $T_2' = 5.4 \times 10^{-9}$ sec $K^2 T^{-2}$ and is in remarkably good agreement, both in magnitude and temperature dependence, with calculations[17] based on spectral diffusion due to interactions between two-level systems. The dependence of the decay on the input level of the generating pulses is only partly understood in terms of propagation effects and the reexcitation or deexcitation of two-level systems during successive passes across the sample.

The three-pulse echo decays nonexponentially but with an initial decay time of approximately 100 μsec at 18 mK and 0.69 GHz. This value is in reasonably good agreement with a calculation of the direct process, using $\gamma_L = 1.5$ eV. The nonexponential decay and its temperature dependence are in semiquantitative agreement with the calculated effect of spectral diffusion. Further evidence for spectral diffusion comes from the increased decay rate for larger values of τ_{12}. The contributions from two-level systems with different relaxation rates and/or a phonon bottleneck are difficult to assess without further measurements.

The observation of phonon echoes provides good support for the existence of intrinsic configurational states in a glass. In addition, phonon echoes serve as a powerful probe of the dynamics of those two-level systems at very low temperatures. At the present time, they yield the only direct measurement of the deformation potential γ, rather than the product $\tilde{n}\gamma^2$. They also provide a sensitive probe in a regime of relaxation times where other techniques, such as direct measurement of spectral linewidth, are difficult to use.

ACKNOWLEDGMENTS

We would like to thank S. L. McCall, P. Hu, and L. R. Walker for a number of discussions and W. H. Haemmerle for technical assistance.

[1] R. C. Zeller and R. O. Pohl, Phys. Rev. B 4, 2029 (1971).
[2] R. B. Stephens, Phys. Rev. B 13, 852 (1976), and references therein.
[3] J. C. Lasjaunias, A. Ravex, M. Vandorpe, and S. Hunklinger, Solid State Commun. 17, 1045 (1975).
[4] P. W. Anderson, B. I. Halperin, and C. M. Varma, Philos. Mag. 25, 1 (1972).
[5] W. A. Phillips, J. Low Temp. Phys. 7, 351 (1972).
[6] J. Jäckle. Z. Phys. 257, 212 (1972).
[7] B. Golding, J. E. Graebner, B. I. Halperin, and R. J. Schutz, Phys. Rev. Lett. 30, 223 (1973).
[8] S. Hunklinger, W. Arnold, S. Stein, R. Nava, and K. Dransfeld, Phys. Lett. A 42, 253 (1972).
[9] B. Golding, J. E. Graebner, and R. J. Schutz, Phys. Rev. B 14, 1660 (1976).
[10] J. E. Graebner and B. Golding (unpublished).
[11] S. Hunklinger and W. Arnold, in *Physical Acoustics*, edited by R. N. Thurston and W. P. Mason (Academic, New York, 1976), Vol. 12.
[12] B. Golding, IEEE Trans. Sonics Ultrason. SU24, 692 (1977).
[13] E. L. Hahn, Phys. Rev. 80, 580 (1950).
[14] I. D. Abella, N. A. Kurnit, and S. R. Hartmann, Phys. Rev. 141, 391 (1966).
[15] B. Golding and J. E. Graebner, Phys. Rev. Lett. 37, 852 (1976).
[16] A discussion of the possibility of observing phonon echoes in a glass has recently come to our attention: U. Ch. Kopvillem, Ukr. Fiz. Zh. 21, 1215 (1976).
[17] J. L. Black and B. I. Halperin, Phys. Rev. B 16, 2879 (1977).
[18] B. I. Halperin, in *The Glass Transition and the Nature of the Glassy State*, edited by M. Goldstein and R. Simha (Ann. N.Y. Academy of Sciences, New York, 1976), Vol. 279, p. 173.
[19] R. P. Feynman, F. L. Vernon, and R. W. Hellwarth, J. Appl. Phys. 28, 49 (1957).
[20] J. Joffrin and A. Levelut, J. Phys. (Paris) 36, 811 (1976).

[21]L. Allen and J. H. Eberly, *Optical Resonance of Two-Level Atoms* (Wiley, New York, 1975).
[22]S. L. McCall and E. L. Hahn, Phys. Rev. 183, 457 (1969).
[23]N. S. Shiren, Phys. Rev. B 2, 2471 (1970).
[24]B. Golding and J. E. Graebner, Bull. Am. Phys. Soc. 22, 310 (1977).
[25]J. E. Giraebner and B. Golding, *Proceedings of the International Conference on Lattice Dynamics, Paris, September 1977*, edited by M. Balkanski (Flammarion, Paris, 1978), p. 464.
[26]B. Golding and J. E. Graebner (unpublished).
[27]W. B. Mims, Phys. Rev. 168, 370 (1968); also, in *Electron Paramagnetic Resonance*, edited by S. Geschwind (Plenum, New York, 1972).
[28]J. E. Graebner, Rev. Sci. Instrum. 46, 571 (1975).
[29]A. L. Bloom, Phys. Rev. 98, 1105 (1955).
[30]R. H. Dicke, Phys. Rev. 93, 99 (1954).
[31]W. B. Mims, Rev. Sci. Instrum. 36, 1472 (1965).
[32]F. A. Hopf, Phys. Rev. A 2, 195 (1970).
[33]E. L. Hahn, N. S. Shiren, and S. L. McCall, Phys. Lett. A 37, 265 (1971).
[34]J. R. Klauder and P. W. Anderson, Phys. Rev. 125, 912 (1962).
[35]P. Hu and S. R. Hartmann, Phys. Rev. B 9, 1 (1974).
[36]P. Hu and L. R. Walker, Solid State Commun. 24, 813 (1977).